Surface Modification of TiO2 Nanoparticles For Photochemical Reduction of Nitrobenzene

ARTICLE *in* ENVIRONMENTAL SCIENCE AND TECHNOLOGY · SEPTEMBER 2000

Impact Factor: 5.33 · DOI: 10.1021/es001109+

3 AUTHORS, INCLUDING:

Tijana Rajh
Argonne National Laboratory
176 PUBLICATIONS **7,503** CITATIONS
SEE PROFILE

Marion Charlotte Thurnauer
Argonne National Laboratory
148 PUBLICATIONS **6,314** CITATIONS
SEE PROFILE

Environ. Sci. Technol. **2000**, *34,* 4797−4803

Surface Modification of TiO_2 Nanoparticles For Photochemical Reduction of Nitrobenzene

OLGA V. MAKAROVA,* TIJANA RAJH, AND MARION C. THURNAUER

Chemistry Division, Argonne National Laboratory, Argonne, Illinois 60439

AMY MARTIN, PATRICIA A. KEMME, AND DONALD CROPEK

CN-E, USA CERL, Champaign, Illinois 61826

The effects of surface modification of nanocrystalline titanium dioxide (TiO_2) with specific chelating agents on photocatalytic degradation of nitrobenzene (NB) was investigated in order to design a selective and effective catalyst for removal of nitroaromatic compounds from contaminated waste streams. Mechanisms of NB adsorption and photodecomposition were investigated using infrared absorption and electron paramagnetic resonance spectroscopy. Liquid chromatography and gas chromatography/mass spectrometry were used for byproduct analyses. Arginine, lauryl sulfate, and salicylic acid were found to bind to TiO_2 via their oxygen-containing functional groups. Modification of the TiO_2 surface with arginine resulted in enhanced NB adsorption and photodecomposition, and compared to unmodified TiO_2. The initial quantum yield for photodegradation of NB in this system was found to be $\Phi_{init} = 0.31$ as compared to the one obtained for Degussa P25 of $\Phi_{init} = 0.18$. NB degradation followed a reductive pathway over arginine-modified TiO_2 and was enhanced upon addition of methanol. No degradation of arginine was detected under the experimental conditions. Arginine improved the coupling between NB and TiO_2 and facilitated the transfer of photogenerated electrons from the TiO_2 conduction band to the adsorbed NB. These results indicate that surface modification of nanocrystalline TiO_2 with electron-donating chelating agents is an effective route to enhance photodecomposition of nitroaromatic compounds.

Introduction

Nitroaromatic compounds such as nitrobenzene, 2,4-dinitrotoluene, and 2,4,6-trinitrotoluene are of special interest to the U.S. Army since they are found in waste streams generated from production, storage, and demilitarization of munitions (*1, 2*). In these waste streams, the nitroaromatic compound usually contributes the energetic or toxic characteristic of the waste but is frequently not the most abundant compound present. Selective decomposition of the nitroaromatics is desirable to increase the rate of remediation and to allow reuse and recycle of the less hazardous constituents. Semiconductor photocatalysis has proven to be a promising technology for the removal of various organic pollutants, including nitroaromatic compounds, from groundwater and waste streams (*3*−*10*). Excitation of the semiconductor with light energy greater than its band gap generates electron hole pairs that can be exploited in various redox processes at the semiconductor/solution interface. The rapid recombination of the photogenerated electron hole pairs due to the small charge separation distances within the particle and the nonselectivity of the system are the main problems that limit the utility of photocatalysis. To prevent rapid electron hole recombination, the charge separation distance can be increased by introducing a deeper trapping site outside the semiconductor particle. It was suggested that interfacial electron transfer occurs via surface Ti(IV) atoms that, due to coordination with solvent molecules, constitute trapping sites for the conduction band electrons (*11*), while hole transfer occurs via surface oxygen (*12*). Replacing adsorbed solvent molecules and ions by chelating agents, i.e., surface modification, changes the energetic position of such surface states and may significantly change the chemistry occurring at the titanium dioxide (TiO_2) surface. It has been shown recently that surface complexation of nanocrystalline TiO_2 with some benzene derivatives (*13*) and amino carboxylic acids (*14*−*16*) resulted in enhanced reduction properties of photogenerated electrons. Therefore, this work investigates surface modification of TiO_2 particles with specific chelating agents that may enhance both TiO_2 redox properties and adsorption of nitroaromatic compounds in order to develop a useful strategy for selective, photocatalytic removal of nitroaromatics from waste streams.

In this paper, results are presented for the surface modification of TiO_2 colloidal nanoparticles with various chelating agents to enhance the adsorption and decomposition of nitrobenzene (NB) from aqueous systems. NB was chosen as a model system for the more hazardous and toxic nitroaromatics such as DNT and TNT in contaminated aqueous waste streams. The coordination sphere of the surface titanium atoms is incomplete and thus exhibits high affinity to oxygen-containing ligands to form chelating structures. Three groups of compounds were investigated to enhance adsorption of NB: a long chain carboxylic acid (lauryl sulfate) to make the surface of the TiO_2 particles hydrophobic; an amino acid (L-arginine) with a high affinity for hydrogen-bonding and electron-donating properties; and a benzene derivative (salicylic acid) that may form $\pi-\pi$ donor−acceptor complexes. Surface complexation of colloidal TiO_2 nanoparticles with these modification agents and adsorption of NB onto the modified TiO_2 surface were investigated by diffuse reflectance infrared Fourier transform spectroscopy (DRIFT). Electron paramagnetic resonance spectroscopy (EPR) was used to identify the nature of radical species formed, following illumination, at the nanoparticle surface and to study the mechanism of NB photodecomposition. Chemical analysis of the degradation byproducts was performed using high-performance liquid chromatography (HPLC) and gas chromatography/mass spectrometry (GC/MS).

Experimental Section

All chemicals (Aldrich, Milwaukee, WI) were reagent grade and used without further purification. Triply distilled water was used. Oxygen in the reaction vessel was removed by purging with nitrogen.

Colloidal TiO_2 was prepared by dropwise addition of titanium(IV) chloride to cooled water followed by $TiCl_4$ dialysis against distilled water at 4 °C as previously described

* Corresponding author fax: (630)252-9289; e-mail: makarova@anchim.chm.anl.gov.

10.1021/es001109+ CCC: $19.00
Published on Web 09/29/2000

(*14*). The pH of the colloid was 3.5, and the mean particle size of TiO_2 particles was 45 Å. The concentration of TiO_2 was determined from the concentration of the titanium(IV) peroxide complex obtained after dissolving the colloid in concentrated sulfuric acid (*17*).

An aqueous solution of surface modifier (SM) was added to the TiO_2 colloid in an amount that corresponded to the monolayer surface coverage (45-Å size particles have 30% of Ti atoms at the particle surface) and allowed to stand at least 1 h for complete complexation. NB aqueous solution was added to the suspension, and this mixture was allowed to stand in the dark for 1 day to ensure complete equilibrium. The final solution concentrations were $[TiO_2] = 0.1$ M, [SM] $= 3 \times 10^{-2}$ M, and [NB] $= 4 \times 10^{-4}$ M ($\sim$50 ppm).

DRIFT measurements were performed on a Nicolet 510 (Madison, WI) Fourier transform infrared spectrometer equipped with a Spectra-Tech Inc. (Stamford, CT) diffuse reflectance accessory. The resolution for these experiments was 4 cm^{-1}. Typically, 100 scans were averaged for each spectrum. All results are presented as normalized Kubelka–Munk plots. Samples were prepared for DRIFT analysis by filtering through a cellulose membrane (YM 10, Millipore, Bedford, MA), washing with water on the filter, and drying. This sample was mixed with KCl (10 wt % to KCl) prior to analysis. A drop of 0.1 M solution of NB in methanol was added to a dry sample, and the methanol was evaporated to observe the NB absorption peaks superimposed on the TiO_2 spectra.

EPR spectra were recorded on a Varian E-9 EPR spectrometer (Palo Alto, CA). Samples at 10 K were illuminated directly in the spectrometer cavity with a LX 300 W UV xenon lamp (Atlas Specialty Lighting, Tampa, FL) for 1 h. To determine a charge separation at elevated temperatures, a sample was illuminated at 10 K and then warmed in the dark to 80, 120, and 200 K. EPR data were acquired when the sample was cooled to 10 K between each warmup step to obtain a high signal-to-noise ratio. Before illumination, samples were checked for the background EPR signal. The *g* values were calibrated by comparison to the Mn^{2+} standard in the SrO matrix ($g = 2.0012 + 0.0002$) (*18*).

Steady-state illumination of magnetically stirred degassed samples was performed in a cylindrical quartz cell equipped with a water-cooling jacket that was placed 30 cm in front of a LX 300 W UV xenon lamp. Total photonic flux (250–400 nm) in the cell during irradiation was 7.5×10^{-5} einstein min^{-1}. After the fixed time of illumination, the sample was filtered, and the filtrate was analyzed by chromatography. HPLC analyses were done on a Waters LC Module 1 (Milford, MA) with a Supelco ABZ+ column (Bellefonte, PA), 150 mm $\times$ 4.6 mm. The mobile phase was 70% water/ 30% acetonitrile, and the detection wavelength was 254 nm. The aqueous solutions obtained upon filtration of the samples were extracted three times with CH_2Cl_2. The organic extracts were concentrated in conical vials under a stream of nitrogen and analyzed by GC/MS using a Hewlett-Packard 6890 GC/5973 MSD (Palo Alto, CA) equipped with a HP5MS (5% phenyl/ 95% methyl) 30 m $\times$ 0.25 mm capillary column. The oven temperature was programmed as follows: isothermal at 40 °C for 3 min, from 40 °C to 300 °C at 10 °C/min, and isothermal at 300 °C for 1 min.

Results and Discussion

Surface Modification of Colloidal TiO_2 Nanoparticles. The binding of chelating agents onto the surface of TiO_2 was investigated using diffuse reflectance infrared Fourier transform spectroscopy. The structures of the three types of SM are shown in Chart 1.

Samples of SM TiO_2 were carefully washed with water to remove unbound SM. Infrared spectra of bare TiO_2 (curve 1), arginine (curve 2), and arginine-modified TiO_2 (curve 3) are shown in Figure 1a. The spectrum of bare TiO_2 (curve 1) contains a strong absorption band in the region of 3000 cm^{-1} due to the stretching of adsorbed water molecules that covers somewhat weak absorption of surface hydroxyl stretching vibrations at 3600 cm^{-1} and a band in the 1630 cm^{-1} region characteristic of adsorbed water bending. The vibrational modes of the carboxyl group in arginine change upon binding to the TiO_2 surface. The -CO_2 symmetric stretching band at 1428 cm^{-1} in the amino acid zwitterion form (curve 2) is not observed in the spectrum of arginine-modified TiO_2 (curve 3). Instead, a broad band at 1382 cm^{-1} characteristic of -CO_2 symmetric vibrations in carboxylate salts (-COOM) (*19*) has appeared. The asymmetric -CO_2 stretching band in carboxylate salts in the 1600 cm^{-1} region overlaps with the strong bending mode of adsorbed water molecules on TiO_2. In contrast, NH_2 group vibrations of arginine remained unaffected. NH_2 asymmetric and symmetric stretches at 3357 and 3296 cm^{-1}, as well as the first overtone of NH_2 scissoring at 3168 cm^{-1} (*19*), are present in the spectrum of arginine-modified TiO_2 but are shifted toward higher energy due to the absence of hydrogen bonding upon binding to the TiO_2 surface (*15*). Bands in the region of 3000–2800 cm^{-1} and at 1480 cm^{-1} characteristic of NH_3^+ stretches and deformations (*19*) almost disappear due to deprotonization of NH_3^+ upon interaction of arginine with TiO_2. Bands in the 1700–1625 cm^{-1} region due to NH_2 scissor deformations are not distinguishable from the TiO_2 water absorption. The changes observed in the IR spectrum of arginine suggest that arginine binds to the TiO_2 surface via the carboxyl group and that most probably the binding is bidentate as was shown previously for other chelating agents such as acetate (*20*), cysteine (*14*), and alanine (*15*) on TiO_2.

The infrared spectrum of lauryl sulfate is characterized by asymmetric and symmetric CH_2 stretching that appear strongly at 2913 and 2846 cm^{-1}, respectively, and by asymmetric and symmetric stretching bands of the SO_2 group at 1315–1220 and 1180–1075 cm^{-1}, respectively (Figure 2, curve 1) (*19*). The positions of these bands are influenced by different metal ions, and upon interaction with TiO_2, asymmetric and symmetric stretching vibrations of the SO_2 group appear at 1230–1120 and 1080–1025 cm^{-1}, respectively (Figure 2, curve 2), which corresponds to the vibrations in secondary alkyl sulfate salts (*21*).

Addition of salicylic acid to TiO_2 turns the colorless colloid to bright yellow, indicating the formation of a titanium(IV) salicylate charge-transfer complex (*13*). The infrared spectrum of salicylate-modified TiO_2 can be compared to the spectrum of salicylic acid (Figure 2, curves 3 and 4). The stretching vibration of the -OH group of salicylic acid is significantly shifted toward lower frequencies to 2500 cm^{-1}

CHART 1

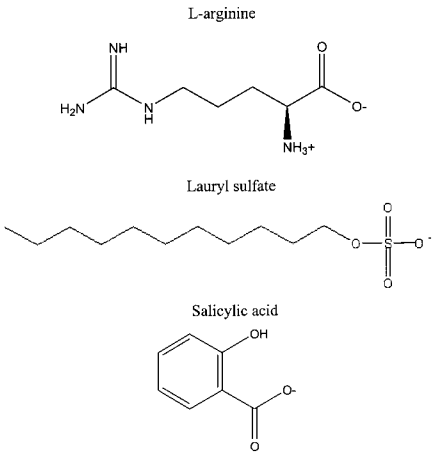

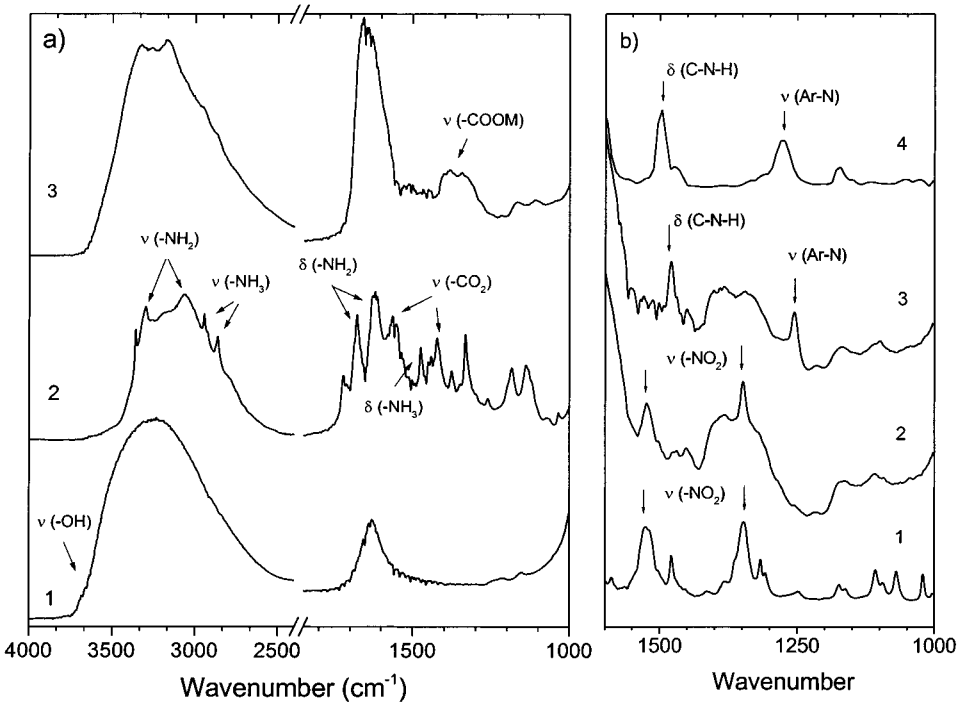

FIGURE 1. (a) Infrared spectra of dried bare nanocrystalline TiO_2 (1), arginine (2), and arginine-modified TiO_2 (3); (b) NB (1), arginine-modified TiO_2 with NB before illumination (2), sample (2) after illumination (3), and aniline (4).

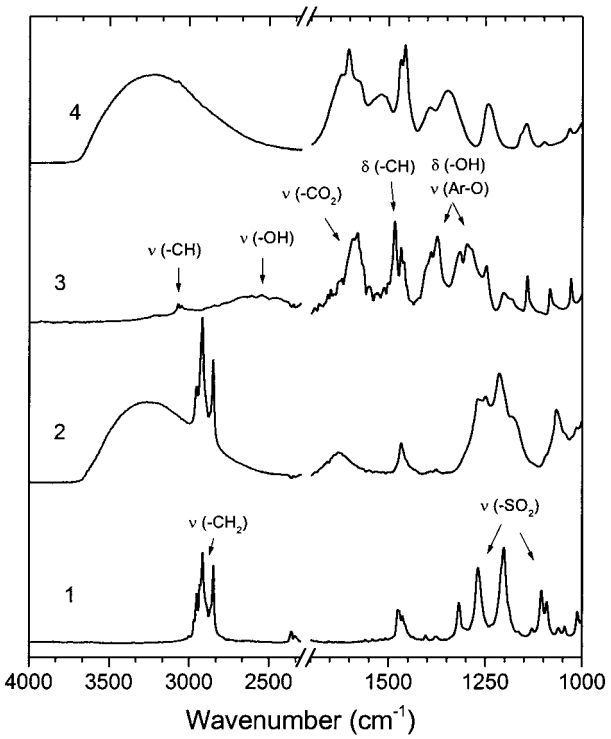

FIGURE 2. Infrared spectra of lauryl sulfate (1), lauryl sulfate-modified TiO_2 (2), salicylic acid (3), and salicylate-modified TiO_2 (4).

due to hydrogen bonding between hydroxyl and adjacent carboxyl groups. When bound to TiO_2, the salicylate modes undergo changes in both carboxyl and hydroxyl group vibrations, while the aryl C−H stretches at 3065 and 1485 cm^{-1} remain unaffected. The -OH stretching band at 2500 cm^{-1} disappears, indicating binding of hydroxyl oxygen to surface titanium atoms. The frequencies of the C−O stretching and C−O−H in-plane bending in the region of 1376−1250 cm^{-1} (*19*) also change upon adsorption. The carboxylate asymmetric stretch at 1580 cm^{-1} shifts to 1522 cm^{-1} and the symmetric stretch at 1394 cm^{-1} appears, indicating formation of the carboxylate salt. This allows the conclusion that both carboxyl and hydroxyl groups of salicylic acid are involved in binding to the TiO_2 surface in agreement with published data (*13*, *22*).

NB Adsorption and Photodecomposition on Surface-Modified TiO_2. The infrared spectrum of NB (Figure 1b, curve 1) contains NO_2 asymmetric and symmetric stretching vibration bands at 1525 and 1350 cm^{-1}; aromatic ring-N stretching bands at 1316 and 1110 cm^{-1}; and benzene ring vibrations at 3070, 1480, and 1070 cm^{-1} (*23*). The NO_2 stretching bands present in the spectrum of NB adsorbed onto arginine-modified TiO_2 (Figure 1b, curve 2). The C−H stretching vibration band of NB at 3070 cm^{-1} shifts to 3000 cm^{-1} (not shown); the bands at 1480, 1316, 1100, and 1070 cm^{-1} become broad and lower in intensity. Similar changes in the ring breathing bands were observed for benzene adsorbed on silica (*24*−*26*) and were attributed to interaction of the ring electrons with silica surface hydroxyl groups. Adsorption of nitroaromatic compounds on clay minerals was studied by various spectroscopic techniques (*27*), where it was concluded that adsorption occurs mainly via formation of an n−π electron donor−acceptor complex between the surface oxygen and the π-system of the ring. Hydrogen bonding or direct coordination of the NO_2 group was found to be negligible in an aqueous environment (*27*). Miller and Wynne-Jones studied the interaction of trinitrobenzene with a variety of electron donors (*28*). They found that aliphatic-type complexes form by electron transfer from an amine nitrogen to either the nitrogen atom of the nitro group or to the electron-deficient π-system of the ring. As mentioned above, the vibrations of the NO_2 group were not affected upon NB adsorption on arginine-modified TiO_2, indicating interaction of the π-system of the NB ring with the arginine amino group. Two mechanisms, formation of an n−π electron donor−acceptor complex and hydrogen bonding, are possible.

NB adsorption on both salicylate- and lauryl sulfate-modified TiO_2 also show NO_2 group stretching bands at 1525 and 1347 cm^{-1} in the IR spectrum (not shown). No other

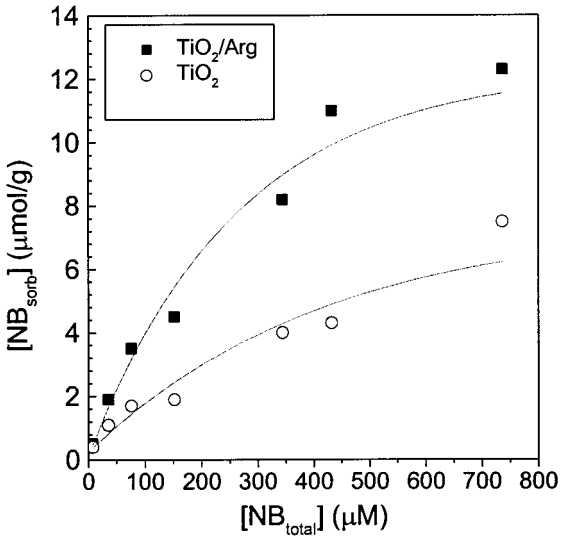

FIGURE 3. Adsorption isotherms of NB measured in aqueous solutions of bare (circles) and arginine-modified TiO_2 (squares).

change in the salicylate-modified TiO_2 IR spectrum is observed upon NB adsorption, possibly due to the overlap of the benzene ring vibrations in NB and salicylate stretching bands. Taking into account the published data of the aromatic donor−acceptor complexes (*28, 29*), a coplanar interaction between the electron deficient π-system of NB (electron acceptor) and the π-system of salicylate (electron donor) is suggested as a reasonable adsorption mechanism of NB on salicylate-modified TiO_2. Adsorption of NB brings some changes in the 1214−1180 cm^{-1} region in the IR spectrum of lauryl sulfate-modified TiO_2. This might be explained by the high sensitivity to the immediate environment, in this case NB, of the methylene rocking, wagging, and twisting modes that appear in this region (*19*). Interaction between NB and the lauryl sulfate surface layer is likely a partitioning mechanism of the NB into this hydrophobic environment, similar to its behavior in reversed-phase chromatography using a long-chain hydrocarbon phase on silica.

HPLC analysis was used to measure the adsorption capacity of the surface modified TiO_2 for NB. Identical volumes of NB solution (1−100 ppm total concentration) were added to identical amounts of bare TiO_2 and each of the surface-modified TiO_2 samples. These samples stood for 1 day for complete adsorption. The experiment is designed to have an excess of surface modified sites versus NB molecules. The sample was centrifuged, and the nonadsorbed NB remaining in the supernatant was measured. It was found that the adsorption of NB increased at all surface-modified TiO_2 as compared with bare TiO_2. The best adsorption was found for arginine-modified (Figure 3) and salicylate-modified TiO_2, while adsorption was smaller in lauryl-modified colloids. This suggests that hydrogen bonding, n−π and π−π interactions result in stronger adsorption of NB as compared with its physical adsorption due to the presence of a hydrophobic environment on the particle surface.

The photocatalytic degradation of NB over bare and arginine-modified nanocrystalline TiO_2 colloid and suspension of Degussa P25 is compared in Figure 4. No direct photolysis of NB was observed under our experimental conditions. HPLC analysis of the filtrates obtained after steady-state illumination of the samples showed the highest NB conversion over arginine-modified TiO_2. The initial quantum yield for photodegradation of NB over arginine-modified TiO_2 is $\Phi_{init} = 0.31$ as compared to the one obtained for unmodified TiO_2 of $\Phi_{init} = 0.15$ and Degussa P25 of $\Phi_{init} = 0.18$. The insert shows GCMS data indicating that reduction

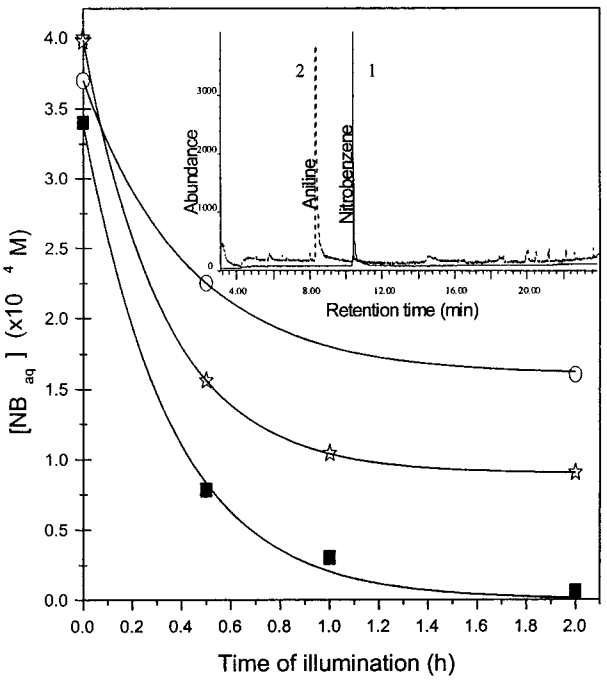

FIGURE 4. Photocatalytic degradation of NB vs time of illumination over bare (circles) and arginine-modified (square) nanocrystalline TiO_2 and Degussa P25 TiO_2 (stars). Inset: Total ion chromatograms from GC/MS analysis of extracts of the initial NB solution (1) and the same solution after illumination with arginine-modified TiO_2 (2).

of NB into aniline is the dominant decomposition pathway using arginine-modified TiO_2 and aniline was the only product of NB photocatalytic decomposition. DRIFT studies showed that the dried arginine-modified TiO_2/NB sample illuminated with Xe lamp or diffuse sunlight only leads to the disappearance of NO_2 stretching bands. Instead, aniline vibration bands at 1480 and at 1253 cm^{-1} assigned to C−N−H bending and to C−N stretching, strongly coupled with ring vibrations (*19*), appear in the spectrum (Figure 1b, curve 3). These vibrations are shifted toward lower frequency compared with aniline alone (Figure 1b, curve 4) due to the aniline adsorption on arginine-modified TiO_2 by hydrogen bonding between the amino groups.

After illumination of both salicylate- and lauryl sulfate-modified samples containing NB, the intensity of NO_2 stretching bands of NB at 1525 and 1347 cm^{-1} decreased. However, no new bands are detected in the IR spectrum (not shown). According to chromatographic analysis, aniline, *p*-benzoquinone, 2-ethylhexanol, phenol, heptanol, and nitrosobenzene are present in the lauryl sulfate-modified TiO_2 solution. These byproducts indicate both NB reduction and oxidation in lauryl sulfate-modified TiO_2, confirming the mechanism previously found for the nitroaromatic compound degradation over Degussa P25 TiO_2 (*3, 6, 30, 31*) and in our experiments over unmodified TiO_2 (*p*-benzoquinone, aniline, phenol, and 3-nitrophenol are major byproducts of NB photodecomposition over bare TiO_2). The presence of the long-chain alcohols indicates that the lauryl sulfate molecule was degraded as well. No byproducts of NB decomposition were found in illuminated salicylate-modified colloid despite an observed decrease in NB concentration. This may be the consequence of a strong irreversible adsorption of NB or its byproducts to colloidal salicylate-modified TiO_2. After 6 h of illumination, the concentration of NB decreased 5-fold, but only dioxolane-type compounds were detected by GC/MS for this system. These are more likely due to the breakdown of the salicylate surface modifier. Further investigation is required to uncover the fate of the

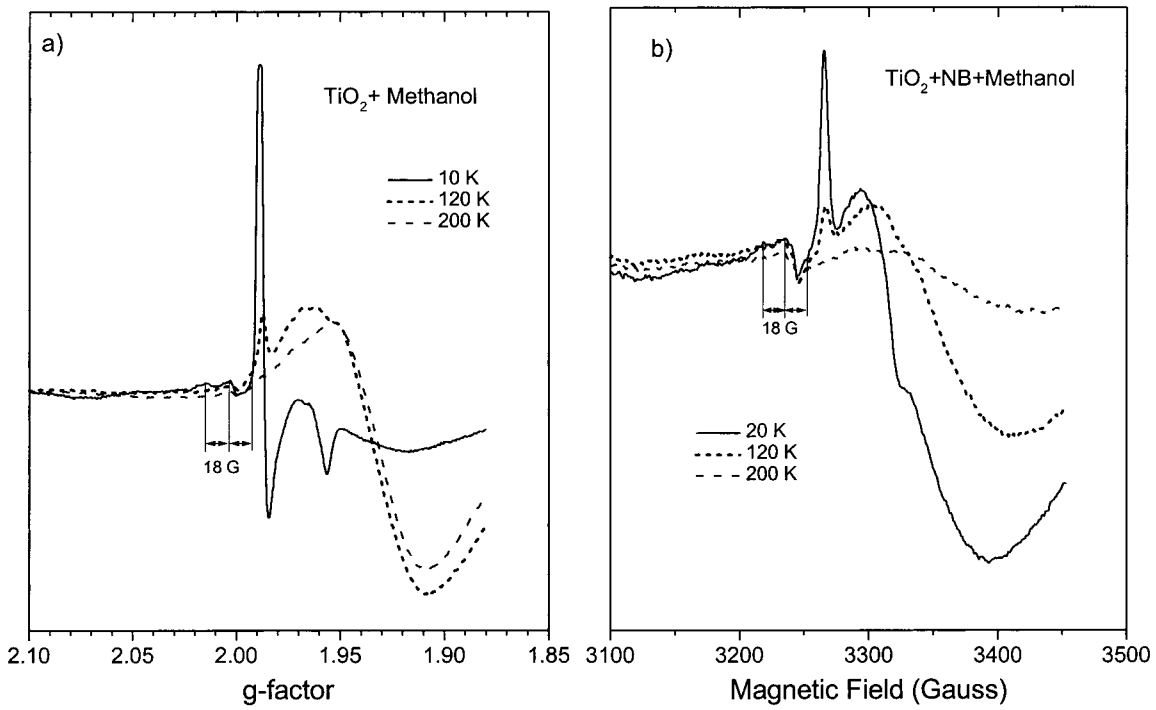

FIGURE 5. (a) EPR (X-band) spectra of degassed aqueous TiO_2 colloids and methanol at 10 K illuminated with a UV xenon lamp (—); temperature raised to 120 K, recorded at 10 K (- - -); and temperature raised to 200 K, recorded at 10 K (— —); (b) EPR (X-band) spectra of degassed aqueous TiO_2 colloids with NB and methanol at 20 K illuminated with a UV xenon lamp (—); temperature raised to 120 K, recorded at 10 K (- - -); and temperature raised to 200 K and recorded at 10 K (— —).

disappearing NB. Complete mineralization of NB combined with salicylate reduction is one possibility.

Degradation in the Presence of Methanol. It was shown that the presence of methanol increases the reductive degradation pathway of nitroaromatic compounds (*32, 33*). Therefore, the photocatalytic degradation of NB in the presence of methanol was also investigated. The involvement of methanol in the degradation process is explained by a current doubling effect on the TiO_2 surface. When the methanol molecule acts as a hole scavenger, a α-hydroxymethyl radical forms. This $^{\bullet}CH_2OH$ radical is capable of injecting an electron into the conduction band of the catalyst. Thus, the absorption of one photon leads to the injection of two electrons into the conduction band of the TiO_2 particle. Addition of methanol to the bare TiO_2 and surface-modified TiO_2 samples results in complete consumption of NB after 3 h of illumination. This is consistent with the enhanced yield of nitroaromatics reduction in the presence of alcohol previously reported (*32, 33*). However, unlike the results published for Degussa P25 catalyst, complex byproducts of NB degradation were observed over bare TiO_2. Initial analysis of the mass spectral data provides no unambiguous library matches. However, the products show evidence of both amino and hydroxyl groups on the aromatic ring, suggesting a complicated mechanism of methanol oxidation and interaction of radical byproducts with NB reduction products. Similar products of NB degradation were detected over lauryl sulfate-modified TiO_2 in addition to products of the lauryl sulfate chain degradation. Aniline is still a main product of NB conversion over arginine-modified colloid; azoxybenzene and azobenzene are also found in the sample filtrate. Addition of methanol again produces no byproducts from NB degradation over salicylate-modified TiO_2.

The results obtained by IR spectroscopy and chromatographic analysis showed that arginine bound to TiO_2 is stable upon illumination and enhances both adsorption and decomposition of NB. Arginine-modified TiO_2 was chosen to study the mechanism of NB photocatalytic decomposition by electron paramagnetic resonance spectroscopy.

EPR Experiments on NB Degradation over Arginine-Modified TiO_2. Illumination of nanocrystalline TiO_2 particles of anatase structure at liquid helium temperatures where diffusion of photogenerated radicals is significantly suppressed leads to the formation of stable photogenerated trapped holes and electrons. These are characterized by spectra composed of two sets of signals: $g > 2$ for trapped holes and $g < 2$ for trapped electrons. The signal for photogenerated holes consists of the oxygen centered radical with $g_x = 2.024$, $g_y = 2.014$, and $g_z = 2.007$ (*34*), while the signal for trapped electrons is composed of axially symmetric signals for bulk Ti(III) in anatase at $g_\perp = 1.988$ and $g_{||} = 1.957$ and for surface Ti(III) with $g_\perp = 1.925$ and $g_{||} = 1.885$, although the latter is much smaller and hardly observable (*12*).

Addition of methanol, an effective hole scavenger and a current doubling agent, to bare TiO_2 at liquid helium temperatures leads to the disappearance of the signal for trapped holes and formation of a triplet signal with hyperfine coupling of H = 18 G. This triplet signal is characteristic of the α-hydroxymethyl radical formed upon the oxidation of methanol. The position of the signal for bulk electrons does not change upon addition of methanol when compared to bare TiO_2 without methanol (not shown), but its intensity is drastically increased, indicating a much lower recombination rate of photogenerated electrons and holes and an enhanced yield of photogenerated charge separation (Figure 5a). When the temperature is raised, the signals for both α-hydroxymethyl radicals and for lattice trapped electrons disappear and convert into a signal for surface trapped electrons, which gains in intensity. This indicates that, in the presence of methanol, all trapped holes and lattice trapped electrons are converted into surface trapped electrons that can perform reductive chemistry. The redox potential of both adsorbed α-hydroxymethyl radicals and lattice trapped electrons is more negative than surface trapped electrons.

Upon addition of NB to this system, one observes the same initial products: α-hydroxymethyl radicals and lattice trapped electrons at 20 K (Figure 5b). When the temperature is raised, α-hydroxymethyl radicals and lattice trapped

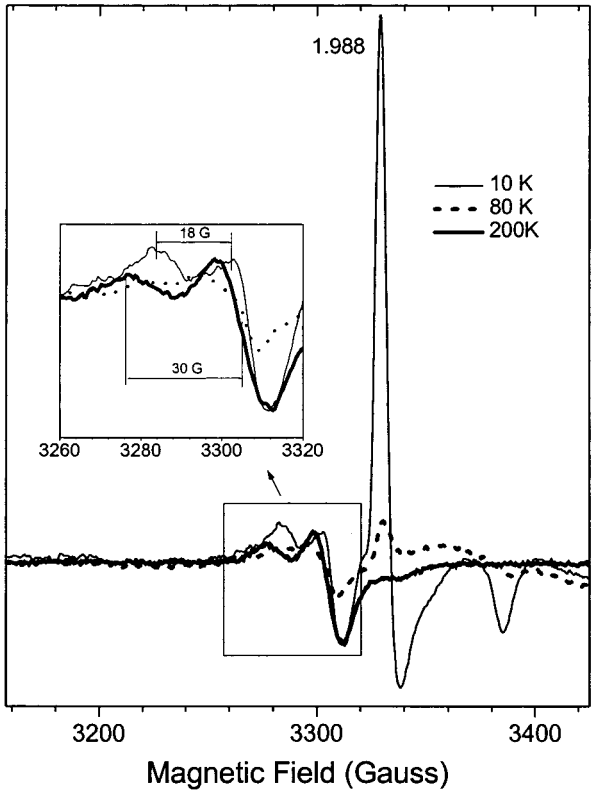

FIGURE 6. EPR (X-band) spectra of degassed aqueous arginine-modified TiO_2 colloids with NB and methanol at 10 K illuminated with UV xenon lamp (—); temperature raised to 80 K, recorded at 10 K (- - -); and temperature raised to 200 K, recorded at 10 K (— —). Insert elucidates the chane in the hyperfine coupling constants upon raising the temperature.

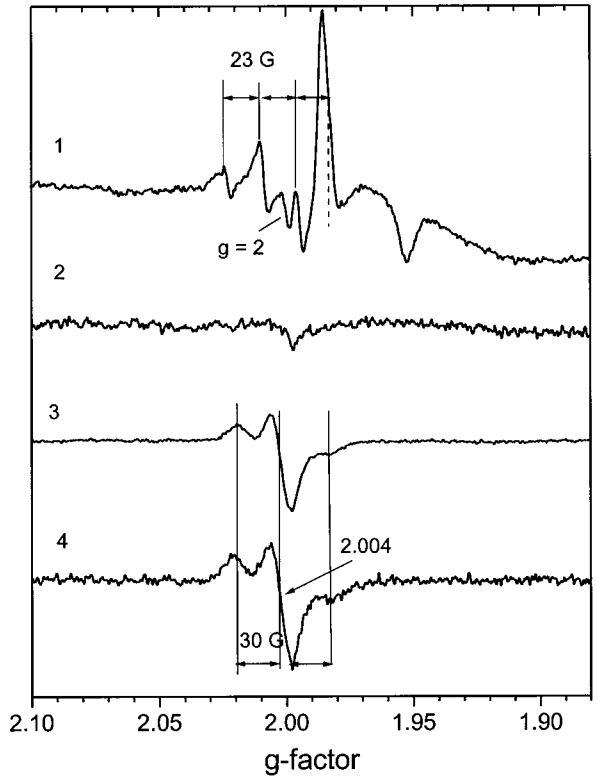

FIGURE 7. EPR (X-band) spectra of degassed arginine-modified TiO_2 colloids at 10 K illuminated with UV xenon lamp (1); temperature raised to 200 K, recorded at 10 K (2); arginine-modified TiO_2 with NB illuminated with UV xenon lamp at 10 K, temperature raised to 200 K, recorded at 10 K (3); and NB reduced with sodium borohydride at room temperature recorded at 20 K (4).

electrons transform into surface electrons, similar to the behavior in the absence of NB. This supports the conclusion previously made from kinetic studies (*35*) that surface electrons, but not α-hydroxymethyl radicals, are responsible for photocatalytic reduction of nitro organics over illuminated TiO_2. At 120 K, the signal for surface trapped electrons slowly decays, but only at 200 K do the surface electrons gain enough diffusion energy to react with NB and the decrease in the signal accelerates. These results indicate that reduction of NB molecules by photogenerated electrons at the TiO_2 surface is kinetically hindered. Therefore, surface modification to bring NB close to the TiO_2 surface can enhance the kinetics and the yield of NB degradation.

EPR spectra of arginine-modified TiO_2 in the presence of methanol and NB at liquid helium temperatures differs from the spectra of the bare TiO_2 sample in the behavior of surface trapped electrons (Figure 6). This signal is almost absent in the spectra at all temperatures, indicating good coupling between TiO_2 and arginine. Most of the electrons are localized as lattice trapped electrons that have a more negative redox potential and are more powerful reducing agents. At elevated temperatures, the lattice electrons migrate to the surface and can be either trapped at the surface sites or react with NB. For the arginine-modified colloid, the majority of the signal for lattice trapped electrons and α-hydroxymethyl radicals has already disappeared at 80 K indicating the consumption of both. Due to the good coupling between TiO_2, arginine, and NB, electrons react with adsorbed NB rather then remain at the surface trapping sites. This result suggests that reduction of NB bound to the TiO_2 surface does not require additional activation energy and has enhanced kinetics of reduction. Without addition of methanol, a similar mechanism of NB reduction was observed but with a smaller yield.

The question of arginine stability upon illumination was also addressed using EPR spectroscopy. Illumination of arginine-modified TiO_2 without methanol formed -NH-C•H-CH_2- radicals detected as a quartet with a splitting constant of 23 G (Figure 7, curve 1) in agreement with published data (*36*). Elevation of the temperature led to the disappearance of the electron and hole signals (Figure 7, curve 2), indicating that radical formation is reversible and no destruction of arginine occurs in agreement with chromatographic data. When NB was added to the arginine-modified sample, the signal for trapped holes was altered, indicating that the -NH- group participates in binding of NB removing this site as a hole trapping center. After increasing the temperature to 200 K, a sharp signal of lattice trapped electrons converts to a triplet with a splitting constant of 30 G (Figure 7, curve 3). A similar spectrum with a *g* factor of 2.004 and a triplet splitting of 30 G assigned to nitrogen-centered radicals C_6H_5N•O_2H was previously observed for reduced NB species (*37*), and it was also obtained in this laboratory upon reduction of NB with sodium borohydride (Figure 7, curve 4).

All the above experiments indicate that surface modifiers with good affinity to the TiO_2 surface and good electron-donating properties significantly enhance the reduction kinetics. Bare nanocrystalline TiO_2 shows modest activity in degrading NB. Modification of TiO_2 with salicylic acid increases the NB adsorption properties of the colloid, but this is not reflected in its ability to photodegrade NB. Although the NB concentration decreases, the lack of byproducts may merely indicate irreversible adsorption rather than degradation. Byproduct analysis also suggests that both salicylate- and lauryl sulfate-modified TiO_2 have unstable surface layers when illuminated. In addition, NB degradation over lauryl sulfate-modified TiO_2 follows both oxidation and reduction pathways. The existence of both reduction and oxidation

pathways reduces the possibilities for the rational design and optimization of a catalyst. For example, when having only one pathway, current doubling agents can be used to convert holes into electrons or vice versa, which in turn doubles the yield of photocatalytic degradation. Due to strong electron donating properties, arginine provides a stable surface layer with a controlled reduction degradation pathway for NB. Arginine also improves the coupling between NB and TiO_2, and electrons from the conduction band of TiO_2 can be transferred to NB without significant activation energy.

Acknowledgments

This work was supported by the U.S. Army Construction Engineering Research Labs, WFO Proposal P-99068. Equipment and facilities for the research done at ANL were developed through the support by the U.S. Department of Energy, Office of Basic Energy Sciences, Division of Chemical Sciences, under Contract W-31-109-Eng-38.

Literature Cited

(1) Urbanski, T. *Chemistry and Technology of Explosives*; Pergamon Press: New York, 1964; Vols. 1−4.
(2) Spanggord, R. J.; Gibson, B. W.; Keck, R. G.; Thomas, D. W.; Barkley, J. J., Jr. *Environ. Sci. Technol.* **1982**, *16*, 229−32.
(3) Pelizzetti, E.; Minero, C.; Piccinini, P.; Vincenti, M. *Coord. Chem. Rev.* **1993**, *125*, 183−94.
(4) Serpone, N. *Res. Chem. Intermed.* **1994**, *20*, 953−92.
(5) Hoffmann, M. R.; Martin, S. T.; Choi, W.; Bahnemann, D. W. *Chem. Rev.* **1995**, *95*, 69−96.
(6) Schmelling, D. C.; Gray, K. A. *Water Res.* **1995**, *29*, 2651−62.
(7) Stafford U.; Gray, K. A.; Kamat, P. V. *Heterog. Chem. Rev.* **1996**, *3*, 77−104.
(8) Schmelling, D. C.; Gray, K. A.; Kamat, P. V. *Water Res.* **1997**, *31*, 1439−47.
(9) Piccinini, P.; Minero, C.; Vincenti, M.; Pelizzetti, E. *Catal. Today* **1997**, *39*, 187−95.
(10) Schmelling, D. C.; Gray, K. A.; Kamat, P. V. *Environ. Sci. Technol.* **1998**, *32*, 971−4.
(11) Kolle, U.; Moser, J.; Gratzel, M. *Inorg. Chem.* **1985**, *24*, 2253−8.
(12) Howe, R. F.; Gratzel, M. *J. Phys. Chem.* **1985**, *89*, 4495−9.
(13) Moser, J.; Punchihewa, S.; Infelta, P. P.; Gratzel, M. *Langmuir* **1991**, *7*, 3012−8.
(14) Rajh, T.; Ostafin, A. E.; Micic, O. I.; Tiede, D. M.; Thurnauer, M. C. *J. Phys. Chem.* **1996**, *100*, 4538−45.
(15) Rajh, T.; Nedeljkovic, J.; Chen, L. X.; Tiede, D. M.; Thurnauer, M. *J. Adv. Oxid. Technol.* **1998**, *3*, 292−8.
(16) Rajh, T.; Nedeljkovic, J. M.; Chen, L. X.; Poluektov, O.; Thurnauer, M. C. *J. Phys. Chem* **1999**, *103*, 3515−9.
(17) Thompson, R. C. *Inorg. Chem.* **1984**, *23*, 1794−8.
(18) Rosenthal, J.; Yarmus, L. *Rev. Sci. Instrum.* **1966**, *37*, 381.
(19) Lin-Vien, D.; Colthup, N. B.; Fateley, W. G.; Grasselli, J. G. *The Handbook of Infrared and Raman Characteristic Frequencies of Organic Molecules*; Academic Press: New York, 1991.
(20) Hug, S. J.; Sulzberger, B. *Langmuir* **1994**, *10*, 3587−97.
(21) Socrates, G. *Infrared Characteristic Group Frequencies*; John Wiley and Sons: New York, 1994.
(22) Tunesi, S.; Anderson, M. *J. Phys. Chem.* **1991**, *95*, 3399−405.
(23) Rao, C. N. R. *Spectroscopy of the Nitro Group*; Feuer, H., Ed.; Interscience Publisher: New York, 1969; Vol. 1.
(24) Egerton, T. A.; Hardin, A. H.; Kozirovski, Y.; Sheppard, N. *J. Catal.* **1974**, *32*, 343−61.
(25) Sayed, M. B.; Cooney, R. P. *J. Colloid Interface Sci.* **1982**, *91*, 552−9.
(26) Ringwald, S. C.; Pemberton, J. E. *Environ. Sci. Technol.* **2000**, *34*, 259−65.
(27) Weissmahr, K. W.; Haderlein, S. B.; Schwarzenbach, R. P.; Hany, R.; Nuesch, R. *Environ. Sci. Technol.* **1997**, *31*, 240−7.
(28) Miller, R. E.; Wynne-Jones, W. F. K. *J. Chem. Soc.* **1959**, 2375−85.
(29) Andrews, L. J. *Chem. Rev.* **1954**, *54*, 713−69.
(30) Low, G.; McEvoy, S. R.; Matthews, R. W. *Environ. Sci. Technol.* **1991**, *25*, 460.
(31) Schmelling, D. C.; Gray, K. A.; Kamat, P. V. *Environ. Sci. Technol.* **1996**, *30*, 2547−55.
(32) Madhavi, F.; Bruton, T. C.; Li, Y. *J. Org. Chem.* **1993**, *58*, 744−6.
(33) Nahen, M.; Bahnemann, D.; Dillert, R.; Fels, G. *J. Photochem. Photobiol. A* **1997**, *110*, 191−9.
(34) Micic, O. I.; Zhang, Y.; Cromack, K. R.; Trifunac, A. D.; Thurnauer M. C. *J. Phys. Chem.* **1993**, *97*, 7277−83.
(35) Ferry, J.; Glaze, W. H. *Langmuir* **1998**, *14*, 3551−5.
(36) Burrell, E. J., Jr. *J. Am. Chem. Soc.* **1961**, *83*, 574−7.
(37) Chachaty, C. *J. Chim. Phys.* **1967**, *64*, 614−26.

Received for review March 17, 2000. Revised manuscript received August 18, 2000. Accepted August 28, 2000.

ES001109+